

**Path Models and MIMO Capacity for Measured  
Indoor Channels at 5.8 GHz**

by

Jeng-Shiann Jiang and Mary Ann Ingram

{jsjiang@ece.gatech.edu, mai@ece.gatech.edu}

School of Electrical and Computer Engineering  
Georgia Institute of Technology

Copyright © 2002 IEEE. Reprinted from the 9th International Symposium on Antenna Technology and Applied Electromagnetics, Aug. 2002. This material is posted here with permission of the IEEE. Internal or personal use of this material is permitted. However, permission to reprint/republish this material for advertising or promotional purposes or for creating new collective works for resale or redistribution must be obtained from the IEEE by sending a blank email message to pubs-permissions@ieee.org. By choosing to view this document, you agree to all provisions of the copyright laws protecting it.

# PATH MODELS AND MIMO CAPACITY FOR MEASURED INDOOR CHANNELS AT 5.8 GHZ

Jeng-Shiann Jiang and Mary Ann Ingram

School of Electrical and Computer Engineering  
Georgia Institute of Technology  
Atlanta, GA 30332-0250, USA  
Email: [gte345k@prism.gatech.edu](mailto:gte345k@prism.gatech.edu), [mai@ece.gatech.edu](mailto:mai@ece.gatech.edu)

## ABSTRACT

Cumulative distribution functions (CDFs) for multiple-input-multiple-output (MIMO) capacities are computed for flat-fading indoor channels at 5.8 GHz. These CDFs are based on two measured channels and on reconstructions of the MIMO channels from path parameters that are estimated based on measured data. The measured data was obtained using the stepped-frequency method of channel sounding in combination with 3-D virtual arrays (also known as synthetic arrays) at both ends of the link. The channels were measured for various antenna element spacings. Several versions of the ESPRIT approach are used to estimate the complex amplitudes, delays, directions-of-arrival (DOAs) and directions-of-departure (DODs) of each path of propagation. One version sequentially estimates each set of parameters. Another version estimates the delays and then jointly estimates the DOAs and DODs, and still other versions jointly estimate all the parameters. A residual estimation error (REE) approach to detecting the number of paths is proposed. We compare the REE results and the capacity CDFs for the different parameter estimation methods and for different antenna element spacings. Sensitivity of the capacity to spacing is observed.

## INTRODUCTION

Performance predictions for wireless links with directional antennas, smart antennas, or multiple-input-multiple-output (MIMO) architectures require channel propagation models that include angle information, generally, at both ends of the link. Path-based models, such as those produced by ray-tracing programs, those estimated based on measured data and those simulated using stochastic geometrical propagation models, are often used to evaluate these links [1,2]. While ray-tracing programs generally assume that a path can undergo more than one reflection or bounce, the stochastic geometrical models normally do not [2]. Furthermore, most MIMO channel sounding experiments have an array at only one end of the link and path angles at the other

end are estimated with the assumption that each path has just one bounce [3].

Exceptions to this are the recent works measuring the so-called double-directional radio channel [4-6]. The authors of [4] estimated sequentially the delays, directions-of-arrival (DOAs) at the receive array, and directions-of-departure (DODs) at the transmit array using ESPRIT [7]. They concluded that a significant amount of power was conveyed by multiply reflected components. In [5], the authors compute cumulative distribution functions (CDFs) of the flat-faded MIMO Shannon capacity from both measured data and from MIMO matrix reconstruction from the double-directional path model. The measured data in [4,5] are taken with a real linear array at one end and a 2-D virtual cross array at the other in a courtyard environment. One of the conclusions in [5] is that there is little change in the outage capacity as a function of antenna spacing.

The joint estimation of delay, DOA, and DOD was proposed in [6]. Unlike the aforementioned sequential estimation, this method jointly estimated all parameters simultaneously by multi-dimensional unitary ESPRIT algorithm, which is a natural extension of 2-D unitary ESPRIT by introducing the simultaneous Schur decomposition (SSC) to replace the eigen-decomposition [8].

The measurement setup of this paper uses virtual 3-D arrays at both ends of the link to measure the MIMO channel matrix for 401 frequency samples over a 500MHz bandwidth in an indoor environment. The measured data is then used two ways. First, it is used to obtain CDFs for the Shannon capacity of a narrowband MIMO link for different antenna element spacings. In contrast to [5], these spacings are varied at both ends of the link in the measured data. These CDFs are based on samples of MIMO capacity in both space and frequency. Second, the data is used to detect the number of paths and estimate the complex amplitudes, delays, DOAs and DODs of those paths.

Various methods are used for path parameter estimation, including sequential and joint estimation. Finally, the path model from each estimation method is used to reconstruct the MIMO channel matrix as a function of frequency and to estimate the corresponding MIMO CDFs.

Therefore, in comparison with [5], this paper treats an indoor channel instead of a courtyard, and focuses more on effects of antenna spacing and the differences in capacity achieved with various path estimation schemes. In particular, we find that MIMO capacity is sensitive to antenna spacing and that the sensitivity is different not only between measured and reconstructed MIMO channels, but also between reconstructed channels that use different parameter estimation schemes. We note that sensitivity to antenna spacing was predicted in [10] for indoor channels with explicit clustering of paths in delay and angle.

Additionally, we propose a new method for detecting the number of paths. This number, which is assumed to be a known value in most parameter estimation algorithms such as MUSIC and ESPRIT, plays a very critical role in the estimation. The traditional detection methods, such as Akaike's information criterion (AIC), are not suitable for this application because the short of number of snapshots [11]. The authors in [5] determine the number of paths based on the relative power decrease between neighboring eigenvalues with additional correction by visual inspection of the Scree graph. In this paper, we propose to detect the number of signals by searching the minimum of the residual estimation error (REE) between the reconstructed and measured signal.

## 1. MIMO CHANNEL MEASUREMENT SYSTEM

As illustrated in Figure 1, our MIMO-channel measurement system is composed of two parts: (1) the HP 85301B stepped-frequency antenna pattern measurement system, which, because of its coherent reference signal, can measure the channel frequency response directly, and (2) the actuator positioning system, employed to emulate the virtual array by moving the antenna to arbitrary pre-programmed locations. Figure 2 shows the photo of the actuator system. The antennas used were biconical.

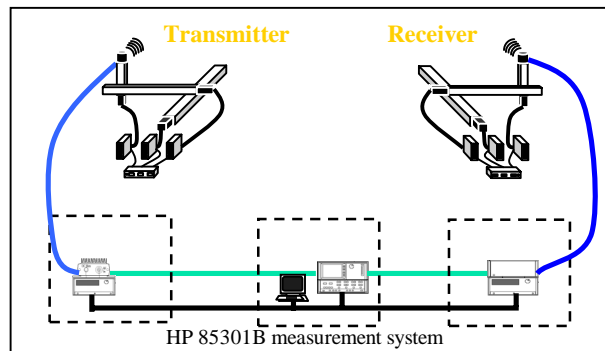


Figure 1. MIMO channel measurement system.

Virtual arrays are used instead of real arrays because: (1) virtual arrays cost less since only two antennas are required, (2) the array shape is arbitrary, so we may investigate the capacity of MIMO systems with various array arrangements, and (3) the measurements are independent of mutual coupling. The mutual coupling effect can be added to the measured data afterwards. The primary drawbacks of virtual arrays are the requirement of a static environment, which implied for us that all the experiments must be carried out after midnight, and the long time required for MIMO measurements because the wideband channel must be sounded for each pair of antenna locations.

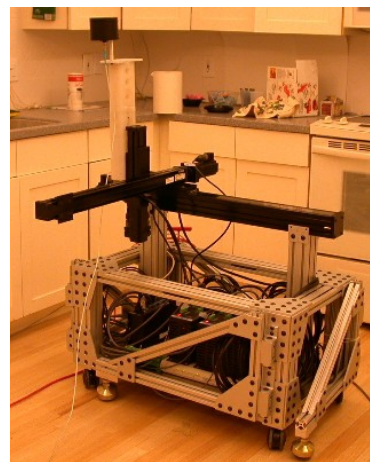


Figure 2. 3D actuator system on mobile platform.

## 2. SIGNAL MODEL

The frequency response in the bi-directional path-based model is represented as

$$h(f, x_R, x_T) = \sum_{i=1}^L \alpha_i e^{j2\pi f \tau_i} e^{jk_{R_i} \cdot \overline{x_R}} e^{jk_{T_i} \cdot \overline{x_T}} + n(f, x_R, x_T), \quad (1)$$

$$\text{where } \begin{cases} f & : \text{ frequency} \\ x_R & : \text{ coordinate of receive antenna} \\ x_T & : \text{ coordinate of transmit antenna} \\ \tau_i & : \text{ delay of path } i \\ k_{R_i} & : \text{ function of DOA of path } i \\ k_{T_i} & : \text{ function of DOD of path } i \\ L & : \text{ Number of paths} \end{cases}$$

The delay steering matrix is

$$\mathbf{A}_\tau = [\mathbf{a}(\tau_1) \quad \mathbf{a}(\tau_2) \quad \mathbf{a}(\tau_3) \quad \cdots \quad \mathbf{a}(\tau_L)], \quad (2)$$

$$\text{where } \mathbf{a}(\tau) = [1 \quad e^{j2\pi\Delta f\tau_1} \quad \cdots \quad e^{j2\pi(N_f-1)\Delta f\tau_1}]^T.$$

When the array is 3D uniform cubical array, the angle steering matrix is

$$\mathbf{A}(\boldsymbol{\theta}, \boldsymbol{\phi}) = [\mathbf{a}(\theta_1, \phi_1) \quad \mathbf{a}(\theta_2, \phi_2) \quad \cdots \quad \mathbf{a}(\theta_L, \phi_L)] \quad (3)$$

$$\mathbf{a}(\theta, \phi) = [1 \quad e^{iu} \quad \cdots \quad e^{i((n_x-1)u+(n_y-1)v+(n_z-1)w)}]^T$$

$$\text{and } \begin{cases} u = \frac{2\pi d_x}{\lambda} \cos \phi \cos \theta \\ v = \frac{2\pi d_y}{\lambda} \cos \phi \sin \theta \\ w = \frac{2\pi d_z}{\lambda} \sin \phi \end{cases}$$

For convenience, the steering matrices of DOA and DOD are denoted as  $\mathbf{A}_R$  and  $\mathbf{A}_T$  in the rest of the paper.

The received array signal is modeled as

$$\mathbf{Y} = \mathbf{A}s + \mathbf{n}, \quad (4)$$

where  $\mathbf{Y}$  is the vector of signals received by the array sensors,  $s$  is the vector of source signals, and  $\mathbf{n}$  is the noise vector. As a result of using the stepped-frequency method of channel sounding, the source signals are pure sinusoids and are therefore perfectly correlated. Smoothing in the various domains is required to decorrelate the source signals prior to the application of ESPRIT.

#### Sequential Estimation Algorithm:

Given the number of frequency samples  $N_f$ , the number of receiver antennas  $N_R$ , and the number of transmitter antennas  $N_T$ , the frequency response  $\mathbf{h}(f, x_R, x_T)$  can be represented as an  $(N_f \times N_R \times N_T)$  three-dimensional matrix, which can further be rearranged to a  $(N_f \times N_R N_T)$  matrix  $\mathbf{h}_f$ . Since  $\mathbf{h}_f$  comprises  $N_R N_T$  snapshots of an  $N_f$ -element frequency array, and it satisfies the rotation-invariance properties, the ESPRIT algorithm can be applied to estimate the delay. Having obtained the delay estimates, the delay steering matrix  $\mathbf{A}_\tau$  in (2) can then

be set up as the beamformer to recover the spatial-channel signal  $\mathbf{h}_{RT}$ , using (5)

$$\mathbf{h}_{RT} = (\mathbf{A}_\tau^H \mathbf{A}_\tau)^{-1} \mathbf{A}_\tau^H \mathbf{h}_f. \quad (5)$$

Likewise, the DOA steering matrix  $\mathbf{A}_R$  can be derived from the DOA estimation result, and subsequently used to recover the signals for DOD estimation corresponding to the specific delay and DOA. Smoothing in each array dimension using overlapping subarrays is done prior to each application of ESPRIT. This is the method of [5].

#### Joint Estimation Algorithm:

If the signal  $\mathbf{h}(f, x_R, x_T)$  is re-organized to a single vector  $\mathbf{h}_{fRT}$  of size  $N_f N_R N_T$ , the signal can be represented as

$$\mathbf{h}_{fRT} = \mathbf{A}_T \otimes \mathbf{A}_R \otimes \mathbf{A}_\tau s, \quad (6)$$

$$\text{where } s = [\alpha_1 \quad \alpha_2 \quad \cdots \quad \alpha_L]^T.$$

The symbol  $\otimes$  in (6) stands for the Kronecker product of the matrices. Snapshots are created by using non-overlapping frequency subarrays and overlapping spatial volume subarrays. Since the signals in each dimension possess the property of rotation-invariance, it is straightforward to apply multi-dimensional ESPRIT to jointly estimate all parameters simultaneously.

With the parameters estimated by ESPRIT, the estimated steering matrix  $\hat{\mathbf{A}}$  can be determined and used to *recover* the sources  $s$  through the pseudo-inverse operation.

$$\hat{s} = (\hat{\mathbf{A}}^H \hat{\mathbf{A}})^{-1} \hat{\mathbf{A}}^H \mathbf{Y}. \quad (7)$$

To compute MIMO capacities based on the path models for various antenna spacings, we must *reconstruct* the received array signal for the new element coordinates. The reconstructed array signals are

$$\hat{\mathbf{Y}} = \hat{\mathbf{A}} \hat{s}. \quad (8)$$

One severe problem with the joint estimation is the huge correlation matrix size caused by multiple dimensions. For instance, if both the transmit and the receive antenna array sizes are  $(3 \times 2 \times 2)$  and the number of frequency samples is 200, the correlation matrix size is as large as 28800, which is intractable with our computer. To overcome this problem, we use the time gating along with non-overlapping, interleaved frequency smoothing to reduce the matrix size. Time gating is the multiplication of the impulse response with a narrow rectangular window, which

will reduce the number of paths and limit the maximum delay. The time-gated signal is then transferred to the frequency domain before the smoothing. In non-overlapping, interleaved frequency smoothing, the frequency spacing between the subarrays is determined by the maximum delay, e.g., the width of the time gate. On the other hand, the bandwidth of the frequency subarray is almost equal to the entire bandwidth. Through this approach, the matrix size is reduced to about 1000 in practice since the number of frequency samples is decreased in the subarray.

### 3. REE NUMBER-OF-PATH DETECTOR

We now describe a new residual estimation error (REE) method to detect the number of signals. The generalized array corresponding to the vector  $\mathbf{Y}$  can be partitioned into two subarrays, corresponding to received signal vectors  $\mathbf{Y}_1$  and  $\overline{\mathbf{Y}}_1$ . The steering matrix  $\mathbf{A}_1$  and  $\overline{\mathbf{A}}_1$  for  $\mathbf{Y}_1$  and  $\overline{\mathbf{Y}}_1$  are also complementary subblocks of  $\mathbf{A}$ . After the parameters are estimated based on some assumed  $\hat{L}$ ,  $\hat{\mathbf{s}}$  is subsequently recovered by  $\mathbf{Y}_1$  and  $\mathbf{A}_1$ , or

$$\hat{\mathbf{s}} = (\hat{\mathbf{A}}_1^H \hat{\mathbf{A}}_1)^{-1} \hat{\mathbf{A}}_1^H \mathbf{Y}_1. \quad (9)$$

$\hat{\mathbf{s}}$  is then used to reconstruct the response of the complementary subarray

$$\hat{\overline{\mathbf{Y}}}_1 = \hat{\mathbf{A}}_1 \hat{\mathbf{s}}. \quad (10)$$

The number of sources can be determined by searching for  $\hat{L}$  that minimizes  $\left\| \hat{\overline{\mathbf{Y}}}_1 - \overline{\mathbf{Y}}_1 \right\|_2$ . This method also works in the noisy environment. The reason is when the number is overestimated, the additional degrees of freedom, which attempt to model the noise samples of the array sensors of  $\mathbf{Y}_1$  in (9) are not suitable for the noise samples of the sensors in  $\overline{\mathbf{Y}}_1$ . All the subsets of  $\mathbf{Y}$  can be used to recover the signal, but one should be careful in selecting the size of the subset in order to obtain the accurate  $\hat{\mathbf{s}}$ . Given the subsets of  $\mathbf{Y}$ , the residual estimation error (REE) is defined as

$$\text{REE} = \sum_{i=1}^M \left\| \hat{\overline{\mathbf{Y}}}_i - \overline{\mathbf{Y}}_i \right\|_2, \quad (11)$$

where  $M$  is the number of subsets. Figure 3 shows an example of the REE number-of-sources detector for the number of paths in a time gate. The distinct jump

in this graph is representative of all the REE graphs used for detection in this paper.

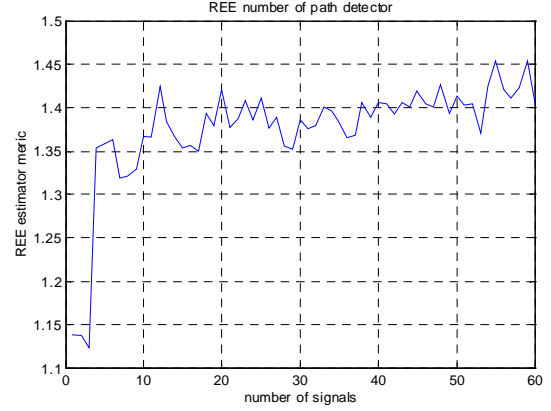


Figure 3. REE number-of-path detector.

### 4. EXPERIMENTAL RESULTS

Two experiments were carried out in Smart Antenna Laboratory situated in Georgia Center of Advanced Telecommunication Technologies (GCATT) building. In Experiment 1, both the transmitter (Tx) and receiver (Rx) array were placed in the same room, so the line of sight (LOS) is available and the distance between the Tx and Rx is 2.56 meters. In Experiment 2, the location of Tx is the same as in previous experiment, while the Rx was moved to another room at a distance of 6 m from the Tx, producing an obstructed LOS. For each experiment, two separate measurements were conducted; one for the parameter estimation, and the other for the direct capacity measurement. The subarray sizes used in the following estimation methods are 200, (3×2×2), (3×2×2), for the delay, DOA, and DOD, respectively. Spatial and frequency smoothing is achieved by averaging the correlation matrices derived from the subarrays. In the capacity measurement, the transmit array is (5×1×1) ULA, while the receive array is (5×5×1) URA. To obtain independent outcomes for the capacity CDF, the frequency spacing is set to 10 MHz in. Accordingly, there are 51 samples over 500 MHz bandwidth. To get spatial samples of capacity, 4-element ULA Tx subarrays and (2×2×1) URA Rx subarrays with specified spacing are extracted from the (5×1×1) ULA and (5×5×1) URA. With this arrangement, we may extract totally 1632 outcomes for capacity CDF. The experiments with different antenna spacing, including 0.25, 0.5, 1, 2, and 3λ, are conducted to explore the capacity sensitivity with the antenna spacing. The details for the measurements are listed in Table 1 and Table 2.

Table 1. Settings for path parameter estimation.

Place:	Smart Antenna Laboratory
Frequency:	5.55 – 6.05 GHz
Frequency samples:	401 pts
Transmitter array:	(4×4×3) Cubical array
Receiver array:	(4×4×3) Cubical array
Transmitter spacing:	0.48 $\lambda$
Receiver spacing:	0.48 $\lambda$

Table 2. Settings for direct capacity measurement

Place:	Smart Antenna Laboratory
Frequency:	5.55 – 6.05 GHz
Frequency samples:	51 pts
Transmitter array:	(5×1×1) ULA
Receiver array:	(5×5×1) URA
Transmitter spacing:	0.25, 0.5, 1, 2, and 3 $\lambda$
Receiver spacing:	0.25, 0.5, 1, 2, and 3 $\lambda$

The following various methods are used to estimate the path parameters.

- (1) *Sequential estimation of delay, DOA, and DOD:* The maximum number of delays is 199. For each delay, the maximum number for DOA estimation is 6 in ESPRIT algorithm with our settings. The maximum number for DOD estimation is also 6. In other words, the maximum allowed number of DOA-DOD pairs is 36 under some specified delay. The number of delays is determined by setting a threshold at 40 dB in delay estimation. REE method is applied to detect the number of signals in angle estimation.
- (2) *Delay estimation. Joint DOA and DOD estimation:* The setting of the method is the same with method (1) except the separate estimation of DOA and DOD is replaced by joint estimation. The maximum number of paths for the joint angle estimation is 72, while we set a limit at 20 when we use REE to detect the number of signals.
- (3) *Joint estimation. Number of paths detected by REE of signals:* The received signal is transferred to the time domain and divided into 40 time gates. Only the time gates whose maximum power is larger than the global maximum power minus 30 dB is considered. The qualified time gate is then transferred back to the frequency domain and joint estimation is conducted. The maximum number of paths is 720 per time gate, but we set the limit at 60 in REE to save time in running the program.
- (4) *Joint estimation. Number of paths detected by REE of power delay profile (PDF):* Detect the number of signals by searching the minimum REE of power delay profile. The rest of the procedure is the same as method (3). The number of signals is usually larger than the one obtained in method (3).
- (5) *Transfer to the time domain by IFFT. Joint DOA and DOD estimation at each time instant:* The received signal is transferred to the time domain. Joint DOA and DOD estimation is carried out

every 2 ns. The setting in REE method is the same with method (2).

### Experiment 1:

Figure 4 depicts the power-angle distribution of DOA and DOD, derived by joint estimation, method (4) for this LOS channel. Only the estimated paths with power larger than maximum power minus 30 dB are shown, and the power is normalized by the minimum power. Therefore, the power of LOS is 30 dB in the figure after the normalization. The elevation angles of DOA and DOD are concentrated around 90° because the Tx and Rx are about the same height in the system.

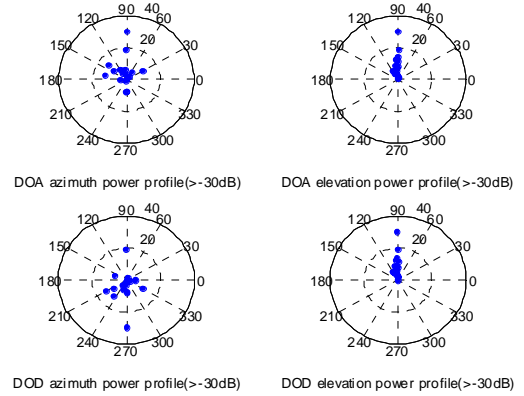


Figure 4. Power-Angle distribution of (a) DOA azimuth angle (b) DOA elevation angle (c) DOD azimuth angle (d) DOD elevation angle.

The power-angle-delay distribution is illustrated in Figure 5, where the height indicates the power of each path.

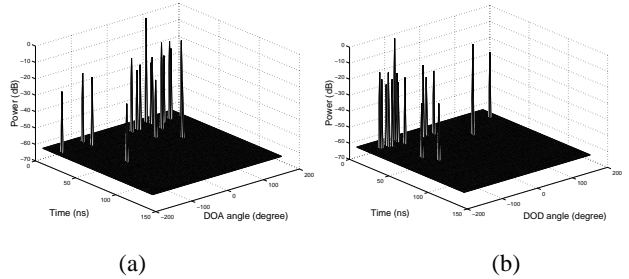


Figure 5. Power-angle-delay distribution of (a) DOA azimuth angle (b) DOD azimuth angle.

The CDFs of the MIMO capacities for the directly measured and reconstructed channels are shown in Figure 6. For each graph, the number in the parentheses in the caption references the parameter estimation method in the list discussed previously. The SNR is assumed to be 30 dB in all cases. For each of the reconstructed channels, the number of paths detected,  $L$ , is shown.

To begin with, we observe that the capacities for the directly measured channel in Figure 6(a) increase with increasing element spacing, with the biggest increase occurring between  $0.25\lambda$  and  $0.5\lambda$ . As a point of reference, we observe the median capacity for  $0.25\lambda$  spacing is about 25 b/s/Hz. The  $0.25\lambda$  CDFs in Figs. 6(c) and 6(f) have almost the same median value as the direct measurement case. However, the  $0.25\lambda$  curves for the other estimation methods are significantly lower.

The increases in capacity with increased antenna spacing vary with estimation method. The sequential method in 6(b) has the largest increases, larger than the direct measurement, while the joint estimation method in 6(d) has the smallest increases. We observe that the number of paths for 6(d) is much smaller than for the other methods. As indicated in 6(e), using the power delay profile for the REE detection yields more paths than REE using the reconstructed measurement vector  $\mathbf{Y}$ .

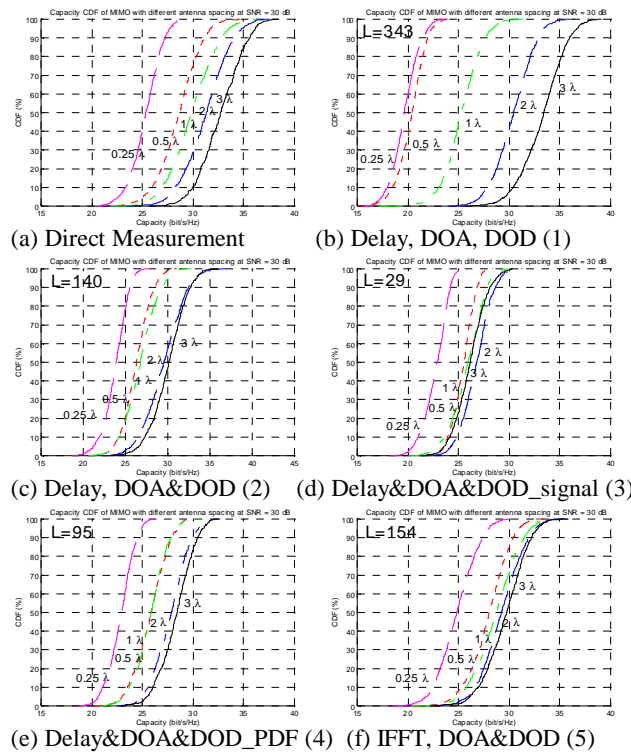


Figure 6. The measured and reconstructed capacities of various parameter-estimation methods.

### Experiment 2:

The power-angle-distribution acquired from the channel in Experiment 2 is shown in Figure 7. Compared with Experiment 1, the number of paths is apparently increased due to the absence of LOS.

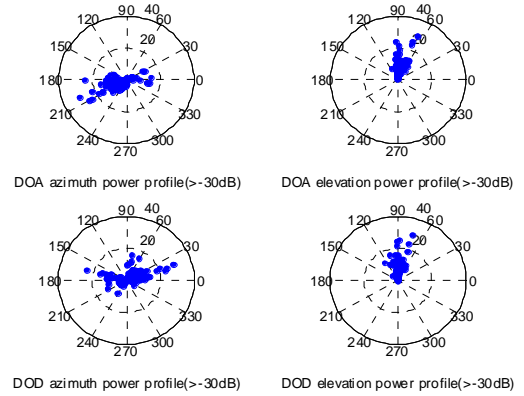


Figure 7. Power-Angle distribution of (a) DOA azimuth angle (b) DOA elevation angle (c) DOD azimuth angle (d) DOD elevation angle.

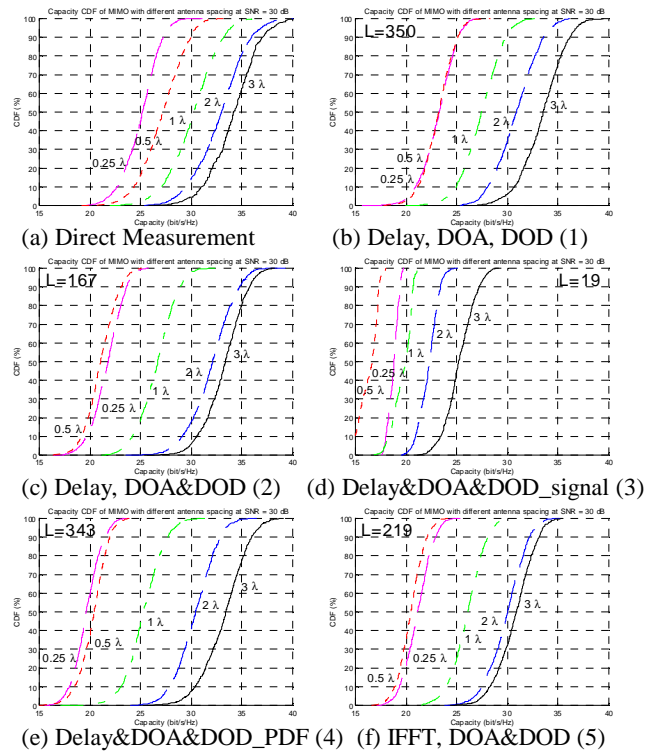


Figure 8. The measured and reconstructed capacities of various parameter-estimation methods.

Figure 8 shows the capacity CDFs for Experiment 2. The median capacities for the reconstructed channels with  $0.25\lambda$  spacing all are lower than the  $0.25\lambda$  direct measurement median. However, the increases in capacity with increased antenna spacing are larger for this non-LOS channel than they were for the LOS channel. The result is that the median capacities for  $3\lambda$  in Figs 8 (b), (c) and (e) are within 2 b/s/Hz of the direct measurement median.

Some possible reasons for the differences between the capacities of the reconstructed channels and the direct measurement channel are

- (1) Near field effect: In the indoor environment, the surrounding scatterers are quite close to the measurement platform, which might make the assumption of far field wave inappropriate in the path-based model.
- (2) Accuracy of estimation results: The estimation results might be distorted due to the small array aperture in our experiments. Also, we compared direct and reconstructed impulse responses for specific TX/RX antenna pairs and observed some non-LOS paths in the reconstructed model appear to have less power than their counterparts in the direct measurement. This may be connected to the reduced power problem discussed in [5].
- (3) Antenna frequency response: The bicone antennas have a non-flat frequency response over the band of our measurements, which could be distorting our delay estimation.

## CONCLUSIONS

We have proposed the residual estimation error (REE) method as a way to estimate the number of paths in a MIMO path-based model. While REE seems to give an unambiguous number of paths for any particular parameter estimation scheme, its result varies widely among the different parameter estimation schemes we considered.

We have also computed flat frequency MIMO capacities for two measured indoor channels and for channels reconstructed from the same original data using various path parameter estimation techniques. We have found that the capacity generally increases as the antenna spacing increases from 0.25 to 3 wavelengths. We also find that the capacities for some parameter estimation methods and some spacings are approximately the same as the capacities of the measured channel matrix. However, for other spacings and other methods, there are significant differences. While possible reasons for the differences are noted, further investigation into the use of path models to evaluate MIMO links seems warranted.

## REFERENCES

- [1] G.G. Raleigh and J.M. Cioffi, "Spatio-temporal coding for wireless communication," *IEEE Trans. Communications*, vol. 46, pp. 357-366, March 1998.
- [2] R.B. Ertel, P. Cardieri, K.W. Sowerby, T.S. Rappaport, and J.H. Reed, "Overview of spatial channel models for

antenna array communication systems," *IEEE Personal Communications Magazine*, pp. 10-22, Feb. 1998.

- [3] U. Martin, "Spatio-temporal radio channel characteristics in urban macrocells," *IEE Proc. Radar, Sonar, and Navigation*, vol. 145, pp. 42-49, 1998.
- [4] M. Steinbauer, D. Hampicke, G. Sommerkorn, A. Schneider, A.F. Molisch, R. Thoma, E. Bonek, "Array measurement of the double-directional mobile radio channel," *IEEE Vehicular Technology Conference*, pp. 1656-1662, 2000.
- [5] A.F. Molisch, M. Steinbauer, M. Toeltsch, E. Bonek, R.S. Thoma, "Capacity of MIMO systems based on measured wireless channels," *IEEE Journal on Selected Areas in Comm.* Vol. 20, NO. 3, pp. 561-569, April 2002.
- [6] A. Richter, D. Hampicke, G. Sommerkorn, R.S. Thoma, "Joint estimation of DOD, time-delay, and DOA for high-resolution channel sounding," *IEEE Vehicular Technology Conference*, pp. 1045-1049, 2000.
- [7] R. Roy, and T. Kailath, "ESPRIT-Estimation of signal parameters via rotational invariance techniques," *IEEE Trans. ASSP*, vol.37, pp. 984-995, July, 1989.
- [8] M. Haardt, and J.A. Nossek, "Simultaneous Schur decomposition of several nonsymmetric matrices to achieve automatic pairing in multi-dimensional harmonic retrieval problems." *IEEE Trans. Signal Processing*, vol. 46, pp. 161-169. Jan. 1998.
- [10] K-H Li, M.A. Ingram, A.V. Nguyen, "Impact of clustering in statistical indoor propagation models on link capacity," *IEEE Trans. on Communications*, pp. 521-523, April 2002.
- [11] A. Kuchar, J. Rossi, E. Bonek, "Directional macro-cell channel characterization from urban measurements," *IEEE Trans. on Antennas and Propagation*, vol. 48, pp. 137-146, Feb. 2000.